Journal of Alzheimer's Disease 63 (2018) 1485–1497
DOI 10.3233/JAD-170943
IOS Press

Total MRI Small Vessel Disease Burden Correlates with Cognitive Performance, Cortical Atrophy, and Network Measures in a Memory Clinic Population

Gargi Banerjee[a,1], Hyemin Jang[b,1], Hee Jin Kim[b,c], Sung Tae Kim[d], Jae Seung Kim[e], Jae Hong Lee[f], Kiho Im[g], Hunki Kwon[h], Jong Min Lee[h], Duk L. Na[b,c], Sang Won Seo[b,c] and David John Werring[a,*]

[a]*Stroke Research Centre, Department of Brain Repair and Rehabilitation, UCL Institute of Neurology and the National Hospital for Neurology and Neurosurgery, London, UK*
[b]*Department of Neurology, Sungkyunkwan University School of Medicine, Samsung Medical Center, Seoul, Republic of Korea*
[c]*Neuroscience Center, Samsung Medical Center, Seoul, Republic of Korea*
[d]*Department of Radiology, Samsung Medical Center, Sungkyunkwan University School of Medicine, Seoul, Republic of Korea*
[e]*Department of Nuclear Medicine, University of Ulsan College of Medicine, Asan Medical Center, Seoul, Republic of Korea*
[f]*Department of Neurology, University of Ulsan College of Medicine, Asan Medical Center, Seoul, Republic of Korea*
[g]*Division of Newborn Medicine, Boston Children's Hospital, Harvard Medical School, Boston, MA, USA*
[h]*Department of Biomedical Engineering, Hanyang University, Seoul, Republic of Korea*

Handling Associate Editor: Daniel Bos

Accepted 30 March 2018

Abstract.
Background: Recent evidence suggests that combining individual imaging markers of cerebral small vessel disease (SVD) may more accurately reflect its overall burden and better correlate with clinical measures.
Objective: We wished to establish the clinical relevance of the total SVD score in a memory clinic population by investigating the association with SVD score and cognitive performance, cortical atrophy, and structural network measures, after adjusting for amyloid-β burden.
Methods: We included 243 patients with amnestic mild cognitive impairment (MCI), Alzheimer's disease dementia, subcortical vascular MCI, or subcortical vascular dementia. All underwent MR and [^{11}C] PiB-PET scanning and had standardized cognitive testing. Multiple linear regression was used to evaluate the relationships between SVD score and cognition, cortical thickness, and structural network measures. Path analyses were performed to evaluate whether network disruption mediates the effects of SVD score on cortical thickness and cognition.

[1]These authors contributed equally to this work.

*Correspondence to: Professor David J. Werring, UCL Stroke Research Centre, Department of Brain Repair and Rehabilitation, UCL Institute of Neurology, Russell Square House, 10 - 12 Russell Square, London WC1B 5EH, UK. Tel.: +44 20 3108 7493; Fax: +44 20 7833 8613; E-mail: d.werring@ucl.ac.uk.

Results: Total SVD score was associated with the performance of frontal (β –4.31, SE 2.09, $p = 0.040$) and visuospatial (β –0.95, SE 0.44, $p = 0.032$) tasks, and with reduced cortical thickness in widespread brain regions. Total SVD score was negatively correlated with nodal efficiency, as well as changes in brain network organization, with evidence of reduced integration and increasing segregation. Path analyses showed that the associations between SVD score and frontal and visuospatial scores were partially mediated by decreases in their corresponding nodal efficiency and cortical thickness.
Conclusion: Total SVD burden has clinical relevance in a memory clinic population and correlates with cognition, and cortical atrophy, as well as structural network disruption.

Keywords: Alzheimer's disease, cerebral small vessel diseases, cognitive dysfunction, magnetic resonance imaging, positron-emission tomography, vascular dementia

INTRODUCTION

Cerebral small vessel diseases (SVD) are common age-related pathologies that affect the brain [1]. There are a number of recognized structural markers of SVD, including white matter hyperintensities (WMH), lacunes, cerebral microbleeds, and MRI-visible perivascular spaces, but their individual correlation with clinical measures, in particular cognition, is often inconsistent [2]. A recently developed "total SVD score" [3] combines these separate imaging markers in an attempt to more closely reflect overall burden, and has shown associations with a number of clinical measures including cognitive performance [4–7], recurrent stroke [8], gait and balance measures [9, 10] and mortality [11]. However, the majority of these studies are in populations with high cardiovascular risk, for example those with hypertension, previous transient ischemic attacks (TIA), or ischemic stroke, with a few in the healthy elderly (aged over 60 years) [5, 7]. Patients with mild cognitive impairment or dementia differ from these patient groups because they more frequently have other coexistent neuropathologies together with SVD, in particular, amyloid-β (Aβ) deposition. It is not known whether the SVD score has clinical relevance in this patient cohort, given that alternate pathologies may make the dominant contribution in these cases.

One method of estimating the impact of SVD has been to use network measures, based on the hypothesis that these SVD processes disrupt the normal connectivity of the brain [12]. The damage caused by SVD extends beyond that visible on brain imaging; for example, "normal appearing" white matter may show diffusion tensor abnormalities in those with SVD [12, 13]. Structural network measures have shown correlations with the presence and progression of cognitive impairment [2, 14] and provide a potential mechanism by which SVD disrupts cognition. Individual structural markers of SVD are also associated with cortical atrophy, another imaging measure that correlates with cognitive dysfunction [15, 16]. The total SVD score provides a unique opportunity to better estimate SVD impact on both brain atrophy and structural network disruption in patient populations with coexisting neuropathologies. Additionally, we hypothesized that vascular damage in the white matter could subsequently cause structural network disruption, and then cortical atrophy [17]; this is supported by evidence showing that the topography of cortical atrophy is similar in regions connected via damaged tracts represented by WMH [18]. Therefore, investigating whether the association between total SVD score and cognition is mediated by structural network disruption and cortical atrophy might help to emphasize the clinical relevance of total SVD score as a marker for overall SVD burden.

Thus, our primary aim was to establish the clinical relevance of the total SVD score in a pooled memory clinic population by reviewing the cognitive associations of total SVD burden; we hypothesized that total SVD score would be particularly associated with "vascular" domains, in particular, frontal and attentional function [19], regardless of clinical diagnosis. Our second objective was to quantify the relative contributions of SVD (as measured by the total SVD score) and brain Aβ (as measured by PiB-PET) to cortical atrophy and structural brain network disruption (as measured by local nodal efficiency, a network parameter that quantifies the importance of each node for communication within a network). Finally, we explored whether any associations between total SVD score and cognition were mediated by structural network disruption, cortical atrophy, or both. In all cases, we wished to review the relative impact of pathology (and in particular

small vessel pathology) rather than diagnosis on our measures of interest.

MATERIALS AND METHODS

Participants

251 subjects with cognitive impairment were prospectively recruited between July 2007 and July 2011. All subjects were clinically diagnosed at the Samsung Medical Center, Seoul, Republic of Korea. In order to be included in the study, patients required a diagnosis of subcortical vascular mild cognitive impairment (MCI), subcortical vascular dementia, probable Alzheimer's disease (AD) dementia, or amnestic MCI.

Subcortical vascular MCI ($n = 67$) was defined using a previously described modification of Petersen's criteria [20]. Subcortical vascular dementia ($n = 70$) was defined clinically using the Diagnostic and Statistical Manual of Mental Disorder Fourth Edition and using imaging criteria proposed by Erkinjuntti et al. [21]. Patients with subcortical MCI and subcortical vascular dementia all had severe WMH on FLAIR, defined as periventricular WMH $\geq$ 10 mm and deep WMH $\geq$ 25 mm, as modified from the Fazekas ischemia criteria [22].

Amnestic MCI ($n = 45$) was defined by Petersen's criteria for MCI. Probable AD dementia ($n = 69$) was defined using National Institute of Neurological and Communicative Disorders and Stroke and the AD and Related Disorders Association criteria [23]. Those with amnestic MCI or AD had WMH that were either minimal (periventricular WMH $<$ 5 mm and deep WMH $<$ 5 mm) or moderate (between minimal and severe WMH classifications).

Patients with territorial (i.e., large vessel) infarctions, WMH due to radiation injury, leukodystrophy, multiple sclerosis, or vasculitis were excluded. While patients with large vessel infarctions were excluded, patients with a clinical history of lacunar stroke or deep intracerebral hemorrhage were not excluded. All patients underwent a clinical interview (for details including cardiovascular risk factors), neurological examination, cognitive assessment by a trained neuropsychologist, blood tests, APOE genotyping, PiB-PET, and structural brain MRI.

This study was approved by Institutional Review Board of the Samsung Medical Center. We obtained written consent from each patient.

Neuropsychological tests

The cognitive assessments were performed by trained neuropsychologists. Participants were tested using the Seoul Neuropsychological Screening Battery (SNSB), which contains tests for attention, language, visuospatial function, verbal and visual memory, and frontal-executive function [24, 25]. Attention score was calculated by summing scores in digit span forward (range 0 to 9) and digit span backward (range 0 to 8). Memory-domain score (memory score) was calculated by summing scores in verbal and visual memory tests; raw scores on Seoul Verbal Learning Test (SVLT) immediate recall (range 0 to 36), delayed recall (range 0 to 12), and recognition (range 0 to 24) and raw scores on Rey–Osterrieth Complex Figure Test (RCFT) immediate recall (range 0 to 36), delayed recall (range 0 to 36), and recognition (range 0 to 24) were all summated. Frontal-executive-domain score (frontal score) was calculated by summing scores in a category word generation task, a phonemic word generation task, and the Stroop color-reading test (range 0 to 120). Raw scores on Korean version of the Boston Naming Test (K-BNT) and RCFT copy test were used as language and visuospatial score, respectively.

MRI acquisition

Standardized T2-weighted, three-dimensional (3D) T1-weighted turbo field echo, 3D fluid-attenuated inversion recovery (FLAIR), T2* gradient echo (GRE), and DTI sequences were acquired for all subjects at the Samsung Medical Center using the same 3.0T MRI scanner (Philips 3.0T Achieva). We acquired 3D T1-weighted turbo field echo MR images using the following parameters: sagittal slice thickness of 1.0 mm, over contiguous slices with 50% overlap; no gap; repetition time (TR) of 9.9 ms; echo time (TE) of 4.6 ms; flip angle of 8°; and matrix size of 240 $\times$ 240 pixels, reconstructed to 480 $\times$ 480 over a field of view (FOV) of 240 mm. The following parameters were used for the 3D FLAIR images: axial slice thickness of 2 mm; no gap; TR 11000 ms; TE 125 ms; flip angle 90°; and matrix size of 512 $\times$ 512 pixels. T2* GRE images were obtained using the following parameters: axial slice thickness of 5.0 mm, inter-slice thickness of 2 mm; TR 669 ms; TE 16 ms; flip angle 18°; and matrix size 560 $\times$ 560 pixels. In whole-brain DT-MRI examinations, sets of axial diffusion-weighted single-shot echo-planar

images were collected with the following parameters: 128×128 acquisition matrix, $1.72 \times 1.72 \times 2$ mm^3 voxels; 70 axial slices; 22×22 cm^2 FOV; TE 60 ms, TR 7696 ms; flip angle 90°; no gap; b-factor of 600 smm^{-2}. Diffusion-weighted images were acquired from 45 different directions using the baseline image without weighting [0, 0, 0]. All axial sections were acquired parallel to the anterior commissure-posterior commissure line.

Structural markers of cerebral small vessel disease (SVD)

Rating was performed by trained individuals blinded to clinical details. Two experienced neurologists (HJK, JHP) rated WMH severity, lacunes, and cerebral microbleeds. WMH severity was rated using FLAIR images using the simplified Fazekas scale [22]; Interrater reliabilities for rating periventricular, deep, and total WMH were between 72.6 and 90.5%. Lacunes were identified and counted using FLAIR, T1-, and T2-weighted images in accordance with STRIVE (STandards for ReportIng Vascular changes on nEuroimaging) criteria [26]. Cerebral microbleeds were rated using the validated Microbleed Anatomical Rating Scale (MARS) [27] using T2* GRE images. Interrater agreement was 78.0% for lacunes and 92.3% for cerebral microbleeds, and consensus was reached in all cases of discrepancy. MRI-visible perivascular spaces in the basal ganglia (BG-PVS) were defined and rated using T2-weighted images by a single rater (GB) using a validated four-point visual rating scale [28, 29].

The SVD score was determined using a previously described four-point scale [3, 5]. This scale awards 1 point for the presence of each of the following (with the maximum possible score being 4): presence of 1 or more lacunes (1 point), presence of 1 or more cerebral microbleeds (1 point), moderate to severe BG-PVS (i.e., presence of >10 BG-PVS; 1 point), and WMH (periventricular WMH Fazekas grade 3 or deep WMH greater than Fazekas grade 2; 1 point) [3].

PET acquisition and analysis

All patients completed a [^{11}C] PiB-PET scan at either the Samsung Medical Center or the Asan Medical Center, using identical settings and a Discovery STe PET/CT scanner (GE Medical Systems, Milwaukee, WI, USA) in both cases. [^{11}C] PiB-PET scanning was performed in 3-dimensional scanning mode that examined 35 slices of 4.25-mm thickness spanning the entire brain. [^{11}C] PiB was injected into an antecubital vein as a bolus with a mean dose of 420 MBq (range 259 to 550 MBq). A CT scan was performed for attenuation correction 60 min after injection. A 30-min emission static PET scan was then initiated. The specific radioactivity of [^{11}C] PiB at the time of administration was more than 1,500 Ci/mmol for patients and the radiochemical yield was more than 35%. The radiochemical purity of the tracer was more than 95% for all PET studies.

PiB-PET images were co-registered to individual MRIs, which were normalized to a Montreal Neurological Institute (MNI)-152 template [30]. The quantitative regional values of PiB retention on the spatially normalized PiB images were obtained by an automated volume of interests (VOIs) analysis using the automated anatomical labeling (AAL) atlas. Data processing was performed using SPM Version 5 (SPM5) within Matlab 6.5 (MathWorks, Natick, MA).

We selected 28 cortical VOIs from left and right hemispheres using the AAL atlas. The cerebral cortical VOIs that were chosen for this study consisted of the bilateral frontal (superior and middle frontal gyri, the medial portion of superior frontal gyrus, the opercular portion of inferior frontal gyrus, the triangular portion of inferior frontal gyrus, supplementary motor area, orbital portion of the superior, middle, and inferior orbital frontal gyri, rectus and olfactory cortex), posterior cingulate gyri, parietal (superior and inferior parietal, supramarginal and angular gyri, and precuneus), lateral temporal (superior, middle and inferior temporal gyri, and heschl gyri), and occipital (superior, middle, and inferior occipital gyri, cuneus, calcarine fissure, and lingual and fusiform gyri). Regional cerebral cortical uptake ratios were calculated by dividing each cortical VOI's uptake ratio by the mean uptake of the cerebellar cortex (cerebellum crus1 and crus2), in order to obtain standardized uptake value ratios (SUVR). Global PiB uptake ratio was calculated from the volume-weighted average uptake ratio of bilateral 28 cerebral cortical VOIs. Patients were considered PiB-positive if their global PiB uptake ratio was greater than 1.5 [31].

Image processing for cortical thickness measurement

The CIVET anatomical pipeline was used to extract cortical thickness (http://mcin-cnim.ca/neuro

imagingtechnologies/civet/) [32]. In brief, using a linear transformation, native MR images were registered to the MNI-152 template [30]. The N3 algorithm was used to correct the images for intensity-based nonuniformities [33] caused by the inhomogeneities in the magnetic field. Then, the registered and corrected images were classified into white matter, grey matter, cerebrospinal fluid, and background using a 3D stereotaxic brain mask and the Intensity-Normalized Stereotaxic Environment for Classification of Tissues (INSECT) algorithm [34]. The surfaces of the inner and outer cortex were automatically extracted using the Constrained Laplacian-based Automated Segmentation with Proximities (CLASP) algorithm [35].

Cortical thickness was defined as the Euclidean distance between the linked vertices of the inner and outer surfaces; there were 40,962 vertices in each hemisphere in native space [35]. The cortical thickness value was spatially normalized using surface-based two-dimensional registration with a sphere-to-sphere warping algorithm. Thus, the vertices of each subject were nonlinearly registered to a standard surface template to compare cortical thickness across subjects [36, 37]. Cortical thickness was subsequently smoothed using a surface-based diffusion kernel in order to increase the signal-to-noise ratio. We chose a 20-mm full-width at half-maximum kernel size to maximize statistical power while minimizing false positives [38]. Using these methods, we obtained the mean cortical thickness values for each lobe.

The presence of extensive WMH in the MRI scans made it difficult to completely delineate the inner cortical surface with the correct topology due to tissue classification errors. To overcome this technical limitation, we automatically defined the WMH region using a FLAIR image and substituted it for the intensity of peripheral, normal-appearing tissue on the high-resolution T1 image after affine co-registration, as described in earlier studies [39].

Network analysis

Network nodes were defined based on the automated anatomical labeling atlas [40], which parcellates the cerebral cortex into 78 areas (39 regions in each hemisphere). Individual T1-weighted images were non-linearly registered to the MNI-152 template [30]. The AAL atlas was transformed from MNI space to T1 native space through inverse transformation with a nearest neighbor interpolation method.

We corrected distortions in DTIs caused by eddy currents and simple head motions using the FSL (FMRIB's Software Library) package diffusion toolbox in the FSL package (http://www.fmrib.ox.ac.uk/fsl/fdt). Diffusion tensor models were estimated, and the fractional anisotropy (FA) was calculated at each voxel. We reconstructed whole-brain white matter fiber tracts in native diffusion space for each subject using the fiber assignment of the continuous tracking algorithm [41] embedded in the Diffusion Toolkit (http://trackvis.org) [42]. We terminated tracking when the angle between two consecutive orientation vectors was greater than the given threshold of 45° or when both ends of the fibers extended outside of the white matter mask generated by the tissue segmentation process [43]. A fiber cutoff filter was applied such that fibers shorter than 20 mm and longer than 200 mm were eliminated.

T1-weighted images were co-registered to the b0 images using the affine registration tool from the FSL package (http://www.fmrib.ox.ac.uk/fsl/%20flirt). Reconstructed whole-brain fiber tracts were inversely transformed into the T1 space, and fiber tracts and AAL-based parcellated regions were located in the same space. Two nodes (regions) were considered to be structurally connected by an edge when at least the endpoints of three fiber tracts were located in these two regions. A threshold for the number of fiber tracts was selected to reduce the risk of false-positive connections due to noise or limitations in the deterministic tractography [43]. The FA value is considered an important index to evaluate fiber integrity [44], and in this study, the mean FA value along all fibers connecting pairs of regions was used to weight the edge. Finally, weighted structural networks represented by symmetric 78 * 78 matrices were constructed for each individual.

Graph theoretical analyses were carried out on weighted connectivity networks using the Brain Connectivity Toolbox (http://www.brain-connectivity-toolbox.net) [46]. To measure network integration (the ability to rapidly combine specialized information from distributed nodes), we calculated the average shortest path length between all pairs of nodes and global efficiency in the network. We also calculated the weighted clustering coefficient, transitivity, and modularity as measures of network segregation (the ability for specialized processing to occur within densely interconnected groups of nodes). Particularly for path analyses, we used *nodal efficiency* as a nodal topological characteristic of structural network, defined using the inverse of

the weighted shortest path length between a given node and all other nodes in the network [46]. The definitions of these network measures and computation methods have been described previously [45–47]. Averaged values of the nodal efficiency in the frontal, temporal, and parietal regions predefined in the AAL atlas were used. Of 243 subjects, we excluded 18 patients for whom the quality of diffusion image (low signal-to-noise ratio) was not sufficient to reconstruct reliable fiber tracts. Thus, network analysis was performed in 225 subjects (Fig. 1).

Statistical analysis

For baseline characteristics, the mean and standard deviation were presented for continuous variables (age, years of education, cognitive and neuropsychological scores, global PiB-SUVR), and frequency and percentage of total population for categorical variables (sex, cardiovascular risk factors, APOE genotype, PiB positivity, components of SVD score). The median and interquartile range was presented for ordinal variables (SVD score). Multiple linear regression analyses (adjusted for age, sex, and education) were used to explore the relationship between SVD score and neuropsychological test results, cortical thickness and structural network measures; linear regression (adjusted as above) was also performed for PiB positivity, to evaluate its relative contribution to cognitive domains significantly associated with SVD score.

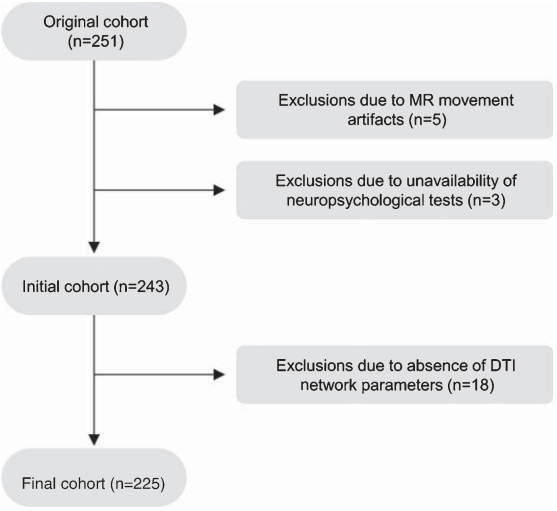

Fig. 1. Flowchart demonstrating inclusion and exclusion of participants included within the study. DTI, diffusion tensor imaging; MR, magnetic resonance.

For cortical thickness analyses, we used a MATLAB-based toolbox (available free online at the University of Chicago website: http://galton.uchicago.edu/faculty/InMemoriam/worsley/research/surfstat/). In order to analyze the localized differences and the statistical map of cortical thickness on the surface model according to increasing SVD score (from 0 to 4), linear regression was performed vertex-by-vertex after controlling for age, sex, education, PiB positivity, and intracranial volume (ICV). The resulting statistical maps were thresholded using a RFT (random field theory) with a p-value of 0.05, after pooling the p-values from the regression analysis.

To evaluate whether alteration of the white matter network mediates the effects of SVD score on cortical thickness and cognition, path analyses were performed after controlling for age, sex, and education. Path analyses were performed for cognitive domains which showed significant associations with total SVD score in multiple linear regression analyses. In the structural equation modeling (SEM), we inserted all possible covariates including SVD score and PiB SUVR as exogenous variables and network measures, cortical atrophy and cognitive score as endogenous variables in the order according to the hypothesis. We selected nodes or cortical regions that were related to frontal-executive (bilateral frontal lobe) and visuospatial (bilateral parietal lobe) function. Path analysis using frontal score as the outcome was performed using mean frontal nodal efficiency and mean frontal thickness as mediators (path analysis A). Path analyses using visuospatial score as the outcomes were performed using mean parietal nodal efficiency/cortical thickness as mediators, respectively (path analysis B). SPSS Amos Version 18.0 software (SPSS, Chicago, IL, USA) was used for all path analyses.

RESULTS

From the original cohort ($n = 251$), 243 patients were included in the cognitive and cortical atrophy analyses, and 225 in the network analyses; reasons for exclusion are provided in Fig. 1. Baseline characteristics for the included cohort are presented in Table 1.

We first investigated the relationship between total SVD score with scores for five cognitive domains (Table 2). Total SVD score was signifi-

cantly associated with deficits in frontal (β –4.31, SE 2.09, $p = 0.040$) and visuospatial (β –0.95, SE 0.44, $p = 0.032$) performance. When looking at associations with PiB positivity, we found that this was significantly associated with deficits in memory (β –14.78, SE 2.69, $p < 0.001$) and language (β –3.46, SE 1.52, $p = 0.024$), with an associative trend between PiB positivity and visuospatial (β –2.28, SE 1.25, $p = 0.070$) performance.

Table 1
Baseline characteristics of participants ($n = 243$)

Demographics	
Mean age, y (SD)	72.2 (8.1)
Sex, female, *n* (%)	143 (58.8)
Education, y, mean (SD)	10.0 (5.4)
Cardiovascular risk factors	
Hypertension, *n* (%)	154 (63.4)
Diabetes mellitus, *n* (%)	48 (19.8)
Hyperlipidemia, *n* (%)	72 (29.6)
Previous clinical history of stroke, *n* (%)	38 (15.6)
APOE genotype†	
ε2 allele carrier, *n* (%)	24/238 (10.1)
ε4 allele carrier, *n* (%)	87/238 (36.6)
Cognitive scores	
MMSE, mean score, (SD)	22.9 (5.1)
CDR_SB, mean score, (SD)	3.7 (3.2)
Neuropsychological scores	
Attention, mean score, (SD)	8.3 (2.4)
Language, mean score, (SD)	35.1 (11.5)
Visuospatial, mean score, (SD)	24.7 (9.7)
Memory, mean score, (SD)	61.3 (20.8)
Frontal, mean score, (SD)	81.3 (45.0)
PiB-PET measures	
Global PiB-SUVR, mean (SD)	1.7 (0.5)
PiB positive, *n* (%)	130 (53.5)
SVD score	
Total SVD score, median (IQR)	2 (0–3)
Lacunes, presence, *n* (%)	140 (57.6)
Cerebral microbleeds, presence, *n* (%)	103 (41.4)
Moderate or severe WMH, presence, *n* (%)	147 (60.5)
Moderate to severe BG-PVS, presence, *n* (%)	71 (29.2)

†APOE genotyping was performed in 238 out of 243 participants. APOE, apolipoprotein E; BG-PVS, basal ganglia-perivascular space; CDR_SB, Clinical Dementia Rating sum or boxes; IQR, interquartile range; MMSE, Mini-Mental Status Examination; PiB, Pittsburgh compound B; SD, standard deviation; SUVR, standardized uptake value ratio; SVD, small vessel disease; WMH, white matter hyperintensities.

We then investigated the relationship between cortical thickness, total SVD score and PiB positivity (Table 3). Total SVD score was negatively associated with mean cortical thickness, globally and regionally. A statistical map of cortical thickness showed that increasing SVD score was associated with cortical thinning in widespread regions, in particular frontal (lateral, medial, inferior) and superior temporal regions (Fig. 2). PiB positivity showed a trend for an overall negative association (β –0.049, SE 0.028, $p = 0.082$) and was regionally correlated with temporal cortical thickness (β –0.090, SE 0.033, $p = 0.007$), with a trend towards a negative association with occipital cortical thickness (β –0.049, SE 0.027, $p = 0.067$).

We next reviewed the associations between total SVD score and structural network measures (Table 4). The most striking finding was that SVD score was highly and significantly correlated with all structural network measures of network strength, while there were no significant associations between PiB positivity and any of the network measures evaluated. Increasing SVD score was associated with a change in network organization, with reduced network integration (increasing path length and lower global efficiency) and increased network segregation (clustering coefficient, transitivity, modularity) (Table 4). Total SVD score was negatively correlated with nodal efficiency across frontal (β –0.182, SE 0.028, $p < 0.001$), temporal (β –0.015, SE 0.002, $p < 0.001$), and parietal (β –0.171, SE 0.030, $p < 0.001$) networks.

We then performed path analyses for frontal and visuospatial scores which showed significant asso-

Table 2
Summary of multiple linear regression models investigating the relationship between neuropsychological composite scores and imaging parameters of interest (SVD score, PiB positivity)

Neuropsychological	SVD score		PiB positivity		R^2
Composite Score	β (SE)	*p* value	β (SE)	*p* value	
Attention	–0.12 (0.10)	0.254	0.19 (0.30)	0.528	0.254
Language	–0.15 (0.54)	0.779	–3.46 (1.52)	0.024	0.151
Visuospatial	–0.95 (0.44)	0.032	–2.28 (1.25)	0.070	0.174
Memory	1.54 (0.95)	0.106	–14.78 (2.69)	<0.001	0.189
Frontal	–4.31 (2.09)	0.040	–8.64 (5.95)	0.147	0.145

Age, sex, and education were entered as covariates for all models. β, unstandardized regression coefficient; PiB, Pittsburgh compound B; SE, standard error; SVD, small vessel disease.

Table 3
Summary of multiple linear regression models investigating the relationship between cortical thickness and imaging parameters of interest (SVD score, PiB positivity)

	SVD score		PiB positivity		R^2
	β (SE)	*p* value	β (SE)	*p* value	
Global cortical thickness	–0.033 (0.010)	0.001	–0.049 (0.028)	0.082	0.138
Frontal cortical thickness	–0.043 (0.011)	<0.001	–0.017 (0.031)	0.567	0.148
Temporal cortical thickness	–0.039 (0.012)	0.001	–0.090 (0.033)	0.007	0.183
Parietal cortical thickness	–0.020 (0.010)	0.052	–0.045 (0.029)	0.122	0.098
Occipital cortical thickness	–0.029 (0.009)	0.003	–0.049 (0.027)	0.067	0.099

Age, sex, and education were entered as covariates for all models. β, unstandardized regression coefficient; PiB, Pittsburgh compound B; SE, standard error; SVD, small vessel disease.

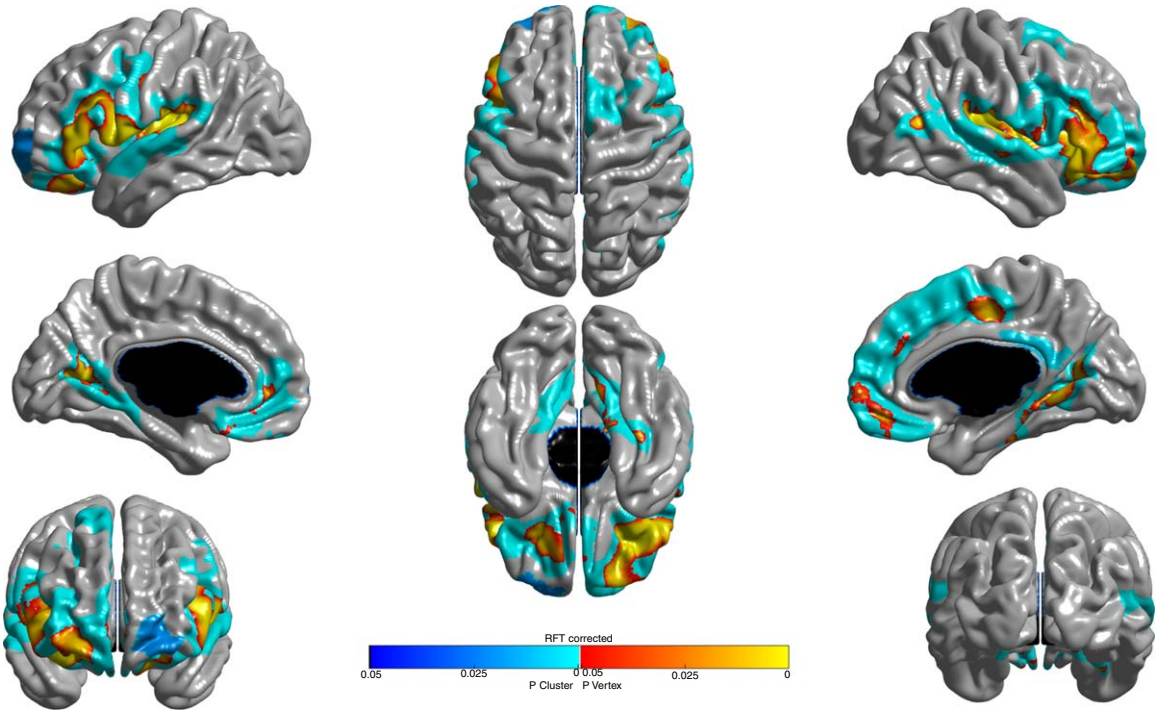

Fig. 2. Statistical map of cortical thickness according to increasing SVD score (range between 0 and 4). Thresholds were applied using RFT with a *p*-value of 0.05. The linear regression model was adjusted for age, sex, education, intracranial volume, and PiB positivity. Increasing SVD score is associated with cortical thinning in widespread regions including the frontal (lateral, medial, inferior) and superior temporal lobes. PiB, Pittsburgh compound B; RFT, random field theory; SVD, small vessel disease (See color image online).

ciations with total SVD score in multiple linear regression analyses. (Fig. 3, Table 5). The path analysis evaluating frontal score demonstrated goodness to fit the data ($\chi^2 = 5.83$, degrees of freedom = 5, $p = 0.323$, comparative fit index = 0.998, root mean square error of approximation = 0.027 (90% CI 0.000 to 0.100)). Increasing SVD score was associated with a decrease in mean frontal nodal efficiency, which itself was associated with a decrease in mean frontal thickness; these two parameters together contributed to impaired frontal-executive function. Decreased frontal nodal efficiency was also associated with reduced frontal score independently of frontal thickness. Increased global PiB SUVR was associated with lower frontal score, independently of frontal nodal efficiency or frontal thickness. The path analysis for visuospatial score showed goodness to fit the data ($\chi^2 = 5.77$, degrees of freedom = 3, $p = 0.124$, comparative fit index = 0.991, root mean square error of approximation = 0.064 (90% CI 0.000 to 0.142)). Increasing SVD score was associated with reduced parietal nodal efficiency, which itself has its effect on visuospatial score via parietal thickness. Reductions in parietal nodal efficiency also had a negative direct effect on visuospatial score, independent of the effect mediated by parietal thick-

Table 4
Summary of multiple linear regression models investigating the relationship between structural network measures and imaging parameters of interest (SVD score, PiB positivity)

	SVD score		PiB positivity		R^2
	β (SE)	*p* value	β (SE)	*p* value	
Shortest path length	0.017 (0.004)	<0.001	0.000 (0.012)	0.974	0.143
Global efficiency	–0.007 (0.001)	<0.001	–0.001 (0.004)	0.781	0.177
Clustering coefficient	0.258 (0.037)	<0.001	0.019 (0.106)	0.858	0.284
Transivity	0.241 (0.033)	<0.001	–0.001 (0.094)	0.990	0.298
Modularity	0.013 (0.002)	<0.001	0.000 (0.006)	0.960	0.270
Mean frontal nodal efficiency	–0.182 (0.028)	<0.001	0.061 (0.079)	0.439	0.317
Mean temporal nodal efficiency	–0.015 (0.002)	<0.001	0.008 (0.006)	0.177	0.274
Mean parietal nodal efficiency	–0.171 (0.030)	<0.001	–0.035 (0.086)	0.683	0.260

Age, sex, and education were entered as covariates. β, unstandardized regression coefficient; PiB, Pittsburgh compound B; SE, standard error; SVD, small vessel disease.

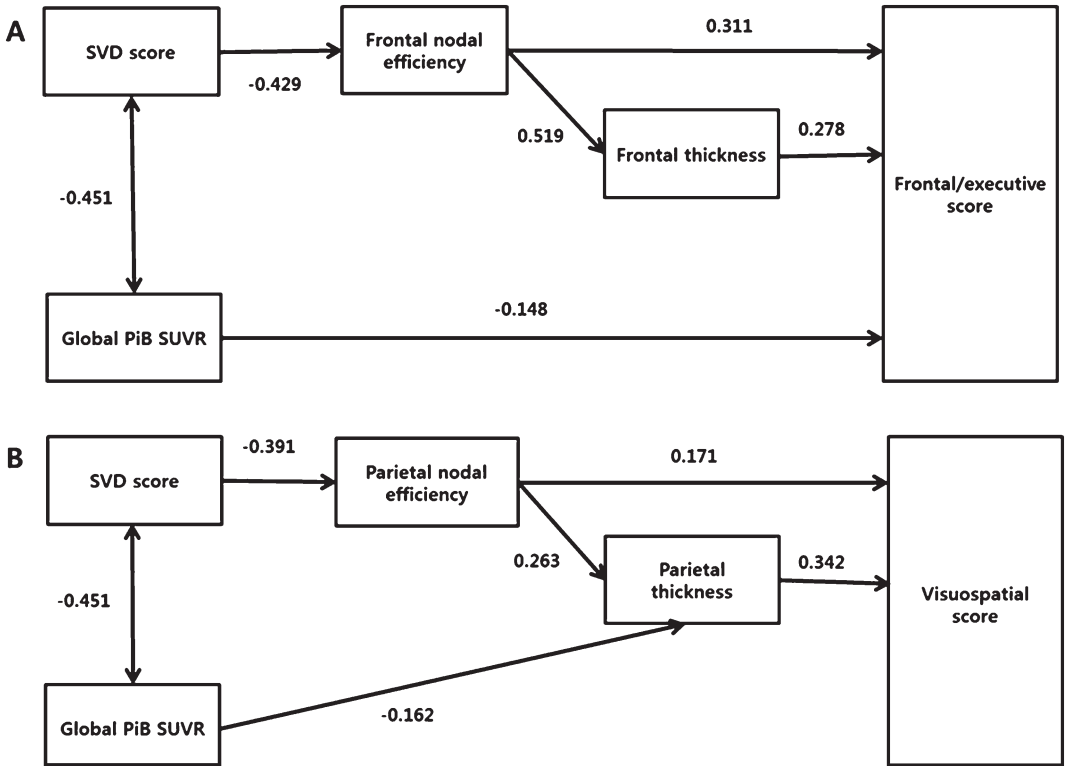

Fig. 3. Schematic representation of the path analyses for frontal-executive (A) and visuospatial (B) scores. SVD score and Aβ burden were entered as predictors. Mean nodal efficiency and mean cortical thickness were entered as mediators. Age, sex, and education were entered as covariates. Numbers on the paths are standardized coefficients that were statistically significant. PiB, Pittsburgh compound B; SUVR, standardized uptake value ratios; SVD, small vessel disease.

ness. Global PiB SUVR had a direct effect on parietal thickness with no effect on parietal nodal efficiency.

DISCUSSION

In a memory clinic population, we report that higher total SVD burden, as measured by a composite SVD score is associated with: (1) reductions in frontal and visuospatial cognitive function; (2) reduced cortical thickness across a number of regions, in particular in frontal and superior temporal regions; (3) altered brain network organization, with reduced integration and increased segregation. The presence of Aβ, as measured by PiB positivity, was associated with impairments in memory and language scores,

Table 5
Effects of SVD score and global PiB SUVR as predictors on frontal (path analysis A) and visuospatial function (path analysis B) through mediators (mean nodal efficiency and mean cortical thickness)

	Path analysis A								
	Mean frontal nodal efficiency			Mean frontal thickness			Frontal score		
	β	SE	*p*	β	SE	*p*	β	SE	*p*
SVD score	–0.429	0.058	<0.001	–0.092	0.075	0.186	0.056	0.064	0.424
Global PiB SUVR	0.018	0.061	0.776	–0.075	0.069	0.215	–0.148	0.055	0.015
Mean frontal nodal efficiency	–	–	–	0.519	0.055	<0.001	0.311	0.072	<0.001
Mean frontal thickness	–	–	–	–	–	–	0.278	0.060	<0.001
	Path analysis B								
	Mean parietal nodal efficiency			Mean parietal thickness			Visuospatial score		
	β	SE	*p*	β	SE	*p*	β	SE	*p*
SVD score	–0.391	0.065	<0.001	–0.090	0.076	0.241	–0.041	0.067	0.560
Global PiB SUVR	–0.052	0.067	0.417	–0.162	0.074	0.018	–0.102	0.066	0.112
Mean parietal nodal efficiency	–	–	–	0.263	0.064	<0.001	0.171	0.066	0.011
Mean parietal thickness	–	–	–	–	–	–	0.342	0.060	<0.001

β, standardized regression coefficient; PiB, Pittsburgh compound B; SE, standard error; SVD, small vessel disease.

and reduced temporal cortical thickness, but did not have an impact upon any of the network measures considered. Additionally, in path analyses for both frontal and visuospatial scores, total SVD score had direct effects upon nodal efficiency, which in turn had negative effects on cortical thickness and cognitive performance.

This is the first time that this total SVD score has been used in a memory clinic cohort. Our mean score is higher than those in previously published cohorts (1.9, compared with calculated means between 0.6 and 1.7) [3–6, 8, 11]. This suggests that there is significant burden of SVD in this cohort, above that observed in ischemic stroke (including lacunar stroke and TIA), hypertensive, and healthy elderly populations. Our results are in keeping with studies in other populations, which have shown an association between total SVD score and cognitive deficits in multiple domains including memory, executive functioning, and information processing speed, as well as general or overall cognitive ability [4, 5] and longitudinal cognitive decline [6]. However, we have extended these observations by demonstrating that total SVD score is also related to cortical thickness and brain network measures, highlighting processes by which structural SVD damage may result in cognitive impairment. Our path analyses show that regional nodal efficiency has both a direct and an indirect (via regional cortical atrophy) effect upon cognitive performance in two different domains, suggesting that subcortical damage intrinsically disrupts network efficiency, leading to cortical atrophy and impairment of tasks requiring cortical integration (i.e., those that rely on "distributed systems" and may be particularly susceptible to "disconnection" [48]). Previous results from this cohort have shown an association between individual structural markers of SVD, specifically WMH and lacunes [45], and cerebral network disruption. However, our results are in contrast with previous work, which did not find any association between total SVD score and cerebral atrophy [3]. This might be because the previous study used a visual rating scale rather than a quantitative measure of cortical thickness.

These results also add to our understanding of how different age-related pathologies may affect the brain. In contrast with the clear and direct impact of total SVD score on cerebral networks, we did not find any association of Aβ burden with structural network measures (again, a finding that has previously been described in this cohort [17]). This may reflect the relative impact that amyloid pathology and small vessel damage have on the white matter tracts that underlie brain network connections. The relatively meagre blood supply of these tracts means that they are particularly vulnerable to hypoxia and the effects of small vessel damage [49]. In contrast, Aβ appears to exert its effects either directly (frontal-executive function) or via cortical thickness (visuospatial score); this may reflect an effect on network "hubs" rather than connections, which are likely to be in the grey matter, and is in keeping with the predominantly cortical distribution of Aβ pathology [50].

The strengths of this study are that this is a well characterized prospective patient cohort, with detailed phenotyping and standardized imaging for all participants. There are also some limitations.

Firstly, these findings may only be applicable to a selected memory clinic population rather than the full spectrum of dementia syndromes that can be encountered in this setting; moreover, our diagnoses were made clinically without pathological verification, and the criteria for patient selection may have resulted in the exclusion of patients with a high burden of both SVD and Aβ pathology. Additionally, we chose to consider the cohort as a whole rather than by diagnosis (as we wished to focus on the impact of SVD as a pathology), which may have made our data more heterogeneous than if each category was considered individually. Secondly, patients underwent PiB-PET at two centers; although the scanner settings and imaging preprocessing methods were identical, we cannot rule out an inter-scanner effect. Thirdly, there are limitations of single diffusion tensor-based deterministic tractography algorithms, because this method cannot detect fiber crossings. Future studies using advanced diffusion acquisition methods, where crossing fibers are included in the model, are warranted to construct enhanced anatomical networks. Finally, the total SVD score has some intrinsic limitations. The interaction between individual markers is likely to be more complex than simple summation of their effects, and the individual markers may have independent effects upon clinical outcomes (as seen with WMH and lacunes [17]), information which is lost once the score is generated.

In summary, total SVD burden has clinical relevance in a memory clinic population, and correlates with cognitive performance of frontal-executive and visuospatial tasks, cortical atrophy in multiple regions, as well as network strength, efficiency, and organization. Further work is needed to confirm the potential of the total SVD score in other dementia syndromes.

ACKNOWLEDGMENTS

GB receives funding from the Rosetrees Trust. HJK receives funding from the National Research Foundation of Korea (NRF-2015R1C1A2A01053 281). SWS receives funding from the Brain Research Program through the National Research Foundation of Korea (NRF-2016M3C7A1913844), Health Technology R&D Project through Korea Ministry of Health & Welfare (HI17C1915), and Korea Ministry of Environment (MOE-2014001360002). DJW receives research support from the Stroke Association, the British Heart Foundation and the Rosetrees Trust. Part of this work was undertaken at UCLH/UCL which receives a proportion of funding from the Department of Health's National Institute for Health Research (NIHR) Biomedical Research Centres funding scheme.

Authors' disclosures available online (https://www.j-alz.com/manuscript-disclosures/17-0943r2).

REFERENCES

[1] Stevens RD, Hannawi Y (2015) Network signatures of age-related cognitive decline. *Neurology* **85**, 16-17.

[2] Banerjee G, Wilson D, Jäger HR, Werring DJ (2016) Novel imaging techniques in cerebral small vessel diseases and vascular cognitive impairment. *Biochim Biophys Acta* **1862**, 926-938.

[3] Staals J, Makin SD, Doubal FN, Dennis MS, Wardlaw JM (2014) Stroke subtype, vascular risk factors, and total MRI brain small-vessel disease burden. *Neurology* **83**, 1228-1234.

[4] Huijts M, Duits A, van Oostenbrugge RJ, Kroon AA, de Leeuw PW, Staals J (2013) Accumulation of MRI markers of cerebral small vessel disease is associated with decreased cognitive function. A study in first-ever lacunar stroke and hypertensive patients. *Front Aging Neurosci* **5**, 72.

[5] Staals J, Booth T, Morris Z, Bastin ME, Gow AJ, Corley J, Redmond P, Starr JM, Deary IJ, Wardlaw JM (2015) Total MRI load of cerebral small vessel disease and cognitive ability in older people. *Neurobiol Aging* **36**, 2806-2811.

[6] Uiterwijk R, van Oostenbrugge RJ, Huijts M, De Leeuw PW, Kroon AA, Staals J (2016) Total cerebral small vessel disease MRI score is associated with cognitive decline in executive function in patients with hypertension. *Front Aging Neurosci* **8**, 301.

[7] Del Brutto VJ, Ortiz JG, Del Brutto OH, Mera RM, Zambrano M, Biller J (2018) Total cerebral small vessel disease score and cognitive performance in community-dwelling older adults. Results from the Atahualpa Project. *Int J Geriatr Psychiatry* **33**, 325-331.

[8] Lau KK, Li L, Schulz U, Simoni M, Chan KH, Ho SL, Cheung RTF, Küker W, Mak HKF, Rothwell PM (2017) Total small vessel disease score and risk of recurrent stroke: Validation in 2 large cohorts. *Neurology* **88**, 2260-2267.

[9] Hatate J, Miwa K, Matsumoto M, Sasaki T, Yagita Y, Sakaguchi M, Kitagawa K, Mochizuki H (2016) Association between cerebral small vessel diseases and mild parkinsonian signs in the elderly with vascular risk factors. *Parkinsonism Relat Disord* **26**, 29-34.

[10] Loos CM, McHutchison C, Cvoro V, Makin SD, Staals J, Chappell F, Dennis MS, van Oostenbrugge RJ, Wardlaw JM (2017) The relation between total cerebral small vessel disease burden and gait impairment in patients with minor stroke. *Int J Stroke*, doi: 10.1177/1747493017730780.

[11] Song TJ, Kim J, Song D, Yoo J, Lee HS, Kim YJ, Nam HS, Heo JH, Kim YD (2017) Total cerebral small-vessel disease score is associated with mortality during follow-up after acute ischemic stroke. *J Clin Neurol* **13**, 187-195.

[12] Lawrence AJ, Chung AW, Morris RG, Markus HS, Barrick TR (2014) Structural network efficiency is associated with cognitive impairment in small-vessel disease. *Neurology* **83**, 304-311.

[13] Tuladhar AM, van Norden AG, de Laat KF, Zwiers MP, van Dijk EJ, Norris DG, de Leeuw FE (2015) White matter integrity in small vessel disease is related to cognition. *Neuroimage Clin* **7**, 518-524.

[14] Tuladhar AM, van Uden IW, Rutten-Jacobs LC, Lawrence A, van der Holst H, van Norden A, de Laat K, van Dijk E, Claassen JA, Kessels RP, Markus HS, Norris DG, de Leeuw FE (2016) Structural network efficiency predicts conversion to dementia. *Neurology* **86**, 1112-1119.

[15] Lambert C, Benjamin P, Zeestraten E, Lawrence AJ, Barrick TR, Markus HS (2016) Longitudinal patterns of leukoaraiosis and brain atrophy in symptomatic small vessel disease. *Brain* **139**, 1136-1151.

[16] Lambert C, Sam Narean J, Benjamin P, Zeestraten E, Barrick TR, Markus HS (2015) Characterising the grey matter correlates of leukoaraiosis in cerebral small vessel disease. *Neuroimage Clin* **9**, 194-205.

[17] Kim HJ, Im K, Kwon H, Lee JM, Kim C, Kim YJ, Jung NY, Cho H, Ye BS, Noh Y, Kim GH, Ko ED, Kim JS, Choe YS, Lee KH, Kim ST, Lee JH, Ewers M, Weiner MW, Na DL, Seo SW (2015) Clinical effect of white matter network disruption related to amyloid and small vessel disease. *Neurology* **85**, 63-70.

[18] Seo SW, Ahn J, Yoon U, Im K, Lee JM, Tae Kim S, Ahn HJ, Chin J, Jeong Y, Na DL (2010) Cortical thinning in vascular mild cognitive impairment and vascular dementia of subcortical type. *J Neuroimaging* **20**, 37-45.

[19] Graham NL, Emery T, Hodges JR (2004) Distinctive cognitive profiles in Alzheimer's disease and subcortical vascular dementia. *J Neurol Neurosurg Psychiatry* **75**, 61-71.

[20] Seo SW, Cho SS, Park A, Chin J, Na DL (2009) Subcortical vascular versus amnestic mild cognitive impairment: Comparison of cerebral glucose metabolism. *J Neuroimaging* **19**, 213-219.

[21] Erkinjuntti T, Inzitari D, Pantoni L, Wallin A, Scheltens P, Rockwood K, Roman G, Chui H, Desmond DW (2000) Research criteria for subcortical vascular dementia in clinical trials. In *Advances in Dementia Research*, Jellinger K, Schmidt R, Windisch M, eds. Springer, Vienna, pp. 23-30.

[22] Fazekas F, Kleinert R, Offenbacher H, Schmidt R, Kleinert G, Payer F, Radner H, Lechner H (1993) Pathologic correlates of incidental MRI white matter signal hyperintensities. *Neurology* **43**, 1683-1689.

[23] McKhann G, Drachman D, Folstein M, Katzman R, Price D, Stadlan EM (1984) Clinical diagnosis of Alzheimer's disease: Report of the NINCDS-ADRDA Work Group under the auspices of Department of Health and Human Services Task Force on Alzheimer's Disease. *Neurology* **34**, 939-944.

[24] Ahn HJ, Chin J, Park A, Lee BH, Suh MK, Seo SW, Na DL (2010) Seoul Neuropsychological Screening Battery-dementia version (SNSB-D): A useful tool for assessing and monitoring cognitive impairments in dementia patients. *J Korean Med Sci* **25**, 1071-1076.

[25] Kang Y, Na DL (2003) *Seoul Neuropsychological Screening Battery (SNSB)*. Human Brain Research & Consulting Co.

[26] Wardlaw JM, Smith EE, Biessels GJ, Cordonnier C, Fazekas F, Frayne R, Lindley RI, O'Brien JT, Barkhof F, Benavente OR, Black SE, Brayne C, Breteler M, Chabriat H, Decarli C, de Leeuw FE, Doubal F, Duering M, Fox NC, Greenberg S, Hachinski V, Kilimann I, Mok V, Oostenbrugge R, Pantoni L, Speck O, Stephan BC, Teipel S, Viswanathan A, Werring D, Chen C, Smith C, van Buchem M, Norrving B, Gorelick PB, Dichgans M; STandards for ReportIng Vascular changes on nEuroimaging (STRIVE v1) (2013) Neuroimaging standards for research into small vessel disease and its contribution to ageing and neurodegeneration. *Lancet Neurol* **12**, 822-838.

[27] Greenberg SM, Vernooij MW, Cordonnier C, Viswanathan A, Al-Shahi Salman R, Warach S, Launer LJ, Van Buchem MA, Breteler MM; Microbleed Study Group (2009) Cerebral microbleeds: A guide to detection and interpretation. *Lancet Neurol* **8**, 165-174.

[28] Doubal FN, MacLullich AM, Ferguson KJ, Dennis MS, Wardlaw JM (2010) Enlarged perivascular spaces on MRI are a feature of cerebral small vessel disease. *Stroke* **41**, 450-454.

[29] Maclullich AM, Wardlaw JM, Ferguson KJ, Starr JM, Seckl JR, Deary IJ (2004) Enlarged perivascular spaces are associated with cognitive function in healthy elderly men. *J Neurol Neurosurg Psychiatry* **75**, 1519-1523.

[30] Collins DL, Neelin P, Peters TM, Evans AC (1994) Automatic 3D intersubject registration of MR volumetric data in standardized Talairach space. *J Comput Assist Tomogr* **18**, 192-205.

[31] Lee JH, Kim SH, Kim GH, Seo SW, Park HK, Oh SJ, Kim JS, Cheong HK, Na DL (2011) Identification of pure subcortical vascular dementia using 11C-Pittsburgh compound B. *Neurology* **77**, 18-25.

[32] Zijdenbos AP, Forghani R, Evans AC (2002) Automatic" pipeline" analysis of 3-D MRI data for clinical trials: Application to multiple sclerosis. *IEEE Trans Med Imaging* **21**, 1280-1291.

[33] Sled JG, Zijdenbos AP, Evans AC (1998) A nonparametric method for automatic correction of intensity nonuniformity in MRI data. *IEEE Trans Med Imaging* **17**, 87-97.

[34] Zijdenbos A, Evans A, Riahi F, Sled J, Chui J, Kollokian V (1996) in *Visualization in Biomedical Computing* Springer, pp. 439-448.

[35] Kim JS, Singh V, Lee JK, Lerch J, Ad-Dab'bagh Y, MacDonald D, Lee JM, Kim SI, Evans AC (2005) Automated 3-D extraction and evaluation of the inner and outer cortical surfaces using a Laplacian map and partial volume effect classification. *Neuroimage* **27**, 210-221.

[36] Lyttelton O, Boucher M, Robbins S, Evans A (2007) An unbiased iterative group registration template for cortical surface analysis. *Neuroimage* **34**, 1535-1544.

[37] Robbins S, Evans AC, Collins DL, Whitesides S (2004) Tuning and comparing spatial normalization methods. *Med Image Anal* **8**, 311-323.

[38] Chung MK, Worsley KJ, Robbins S, Paus T, Taylor J, Giedd JN, Rapoport JL, Evans AC (2003) Deformation-based surface morphometry applied to gray matter deformation. *Neuroimage* **18**, 198-213.

[39] Jeon S, Yoon U, Park JS, Seo SW, Kim JH, Kim ST, Kim SI, Na DL, Lee JM (2011) Fully automated pipeline for quantification and localization of white matter hyperintensity in brain magnetic resonance image. *International Journal of Imaging Systems and Technology* **21**, 193-200.

[40] Tzourio-Mazoyer N, Landeau B, Papathanassiou D, Crivello F, Etard O, Delcroix N, Mazoyer B, Joliot M (2002) Automated anatomical labeling of activations in SPM using a macroscopic anatomical parcellation of the MNI MRI single-subject brain. *Neuroimage* **15**, 273-289.

[41] Mori S, Crain BJ, Chacko VP, van Zijl PC (1999) Three-dimensional tracking of axonal projections in the brain by magnetic resonance imaging. *Ann Neurol* **45**, 265-269.

[42] Wang R, Benner T, Sorensen AG, Wedeen VJ (2007) Diffusion toolkit: A software package for diffusion imaging data processing and tractography. *Proc Intl Soc Mag Reson Med*, Berlin.

[43] Kim MJ, Seo SW, Kim GH, Kim ST, Lee JM, Qiu A, Na DL (2013) Less depressive symptoms are associated with smaller hippocampus in subjective memory impairment. *Arch Gerontol Geriatr* **57**, 110-115.

[44] Beaulieu C (2002) The basis of anisotropic water diffusion in the nervous system - a technical review. *NMR Biomed* **15**, 435-455.

[45] Kim HJ, Im K, Kwon H, Lee JM, Ye BS, Kim YJ, Cho H, Choe YS, Lee KH, Kim ST, Kim JS, Lee JH, Na DL, Seo SW (2015) Effects of amyloid and small vessel disease on white matter network disruption. *J Alzheimers Dis* **44**, 963-975.

[46] Rubinov M, Sporns O (2010) Complex network measures of brain connectivity: Uses and interpretations. *Neuroimage* **52**, 1059-1069.

[47] Bullmore E, Sporns O (2009) Complex brain networks: Graph theoretical analysis of structural and functional systems. *Nat Rev Neurosci* **10**, 186-198.

[48] Dey AK, Stamenova V, Turner G, Black SE, Levine B (2016) Pathoconnectomics of cognitive impairment in small vessel disease: A systematic review. *Alzheimers Dement* **12**, 831-845.

[49] Martinez Sosa S, Smith KJ (2017) Understanding a role for hypoxia in lesion formation and location in the deep and periventricular white matter in small vessel disease and multiple sclerosis. *Clin Sci (Lond)* **131**, 2503-2524.

[50] Stam CJ (2014) Modern network science of neurological disorders. *Nat Rev Neurosci* **15**, 683-695.